Genomic Analysis of Cutaneous CD30-Positive Lymphoproliferative Disorders

Farah R. Abdulla[1], Weiwei Zhang[2], Xiwei Wu[3], Kord Honda[4], Hanjun Qin[3], Hyejin Cho[3], Christiane Querfeld[1], Jasmine Zain[5], Steven Terry Rosen[5], Wing C. Chan[6], Vishwas Parekh[6] and Joo Y. Song[6]

Primary cutaneous CD30$^+$ T-cell lymphoproliferative disorders are the second most common cutaneous lymphomas. According to the World Health Organization, CD30$^+$ T-cell lymphoproliferative disorders include primary cutaneous anaplastic large cell lymphoma (C-ALCL) and lymphomatoid papulosis (LyP) as well as borderline lesions. C-ALCL and LyP are thought to represent two ends of a spectrum of diseases that have different clinical presentations, clinical courses, and prognoses in their classic forms but share the same histology of medium to large CD30$^+$ atypical lymphoid cell infiltrates. Because the behavior of these entities is different clinically and prognostically, we aim to search for oncogenic genomic variants using whole-exome sequencing that drive the development of LyP and C-ALCL. Clinical information, pathology, immunohistochemistry, and T-cell rearrangements on six cases of LyP and five cases of C-ALCL were reviewed to confirm the rendered diagnosis before whole-exome sequencing of all specimens. Both LyP and C-ALCL had recurrent alterations in epigenetic modifying genes affecting histone methylation and acetylation (*SETD2*, *KMT2A*, *KMT2D*, and *CREBBP*). However, they also harbor unique differences with mutations in signal transducer and activator of transcription gene *STAT3* of the Jak/signal transducer and activator of transcription pathway and *EOMES*, a transcription factor involved in lymphocyte development, only noted in C-ALCL specimens. Genomic characterization of LyP and C-ALCL in this series confirms the role of multiple pathways involved in the biology and development of these lymphomatous processes. The identification of similar aberrations within the epigenetic modifying genes emphasizes common potential development mechanisms of lymphomagenesis within lymphoproliferative disorders being shared between LyP and C-ALCL; however, the presence of differences may account for the differences in clinical course.

JID Innovations (2022);**2:**100068 doi:10.1016/j.xjidi.2021.100068

INTRODUCTION

Primary cutaneous CD30$^+$ lymphoproliferative disorders (CD30$^+$LPDs) are a subcategory of cutaneous T-cell lymphoma (CTCL) that includes lymphomatoid papulosis (LyP) and primary cutaneous anaplastic large cell lymphoma (C-ALCL) (Swerdlow et al., 2017). CD30$^+$LPDs are rare, indolent entities with overlapping histology but have different clinical presentations. LyP presents as small subcentimeter self-resolving papules; C-ALCL presents as persisting large tumors (Kempf et al., 2011). C-ALCL and LyP subtypes A and C have histologic overlap with the aggressive entities systemic anaplastic large cell lymphoma (sALCL) and mycosis fungoides (MF) with large cell transformation. Differentiating these entities is challenging, leading to misdiagnosis and treatment with unnecessary chemotherapy in patients with the more indolent CD30$^+$LPDs (Laube et al., 2006). *DUSP22–IRF4* and *NPM1–TYK2* rearrangements can be seen in a subset of LyP and C-ALCL cases (Feldman et al., 2011; Karai et al., 2013; Velusamy et al., 2014) but are not specific to any entity. Thus, there is a critical clinical need to molecularly differentiate indolent CD30$^+$LPD from the aggressive mimics.

RESULTS

Clinical data and pathological features

Six samples of LyP histologic subtypes A and C and five samples of C-ALCL with matched germline tissue were included in this study from the City of Hope National Medical Center (Duarte, CA) and University Hospitals of Cleveland (OH). Patient 1 with LyP has two biopsies at two different time points. The immunophenotypic characteristics of the specimens are provided in Table 1.

[1]*Department of Surgery, City of Hope National Medical Center, Duarte, California, USA;* [2]*Department of Pathology and Microbiology, University of Nebraska Medical Center, Omaha, Nebraska, USA;* [3]*Integrative Genomics Core, City of Hope National Medical Center, Duarte, California, USA;* [4]*Department of Pathology, University Hospitals of Cleveland, Cleveland, Ohio, USA;* [5]*Department of Hematology & Hematopoietic Cell Transplantation, City of Hope National Medical Center, Duarte, California, USA; and* [6]*Department of Pathology, City of Hope National Medical Center, Duarte, California, USA*

Correspondence: Farah R. Abdulla, Department of Surgery, City of Hope National Medical Center, 1500 East Duarte Road, Duarte, California 91010, USA. E-mail: abdullafr@gmail.com

Abbreviations: BI-ALCL, breast implant–associated anaplastic large cell lymphoma; C-ALCL, cutaneous anaplastic large cell lymphoma; CD30$^+$LPD, CD30$^+$ lymphoproliferative disorder; CN, copy number; CTCL, cutaneous T-cell lymphoma; FFPE, formalin-fixed, paraffin-embedded; IHC, immunohistochemistry; LyP, lymphomatoid papulosis; MF, mycosis fungoides; sALCL, systemic anaplastic large cell lymphoma; STAT, signal transducer and activator of transcription

Received 10 February 2021; revised 21 September 2021; accepted 22 September 2021; accepted manuscript published online XXX; corrected proof published online XXX

Cite this article as: JID Innovations 2022;2:100068

Table 1. Histologic Characteristics of Six Cases of LyP and Five Cases of Primary C-ALCL

Case	Sex	DX	Age at Biopsy	CD3	CD4	CD5	CD7	CD8	CD30	TIA-1	GB	Pf	BF1	Gamma	TCR
1a	M	LyP	62	neg	pos	neg	neg	neg	pos	neg	neg	pos	ND	ND	neg
1b	M	LyP	62	pos	pos	neg	neg	neg	pos	ND	ND	ND	ND	ND	ND
2	M	LyP	70	pos	pos	ND	neg	neg	pos	ND	ND	ND	ND	ND	pos
3	F	LyP	54	pos	pos	ND	neg	neg	pos	ND	ND	ND	ND	ND	pos
4	M	LyP	65	pos	pos	ND	neg	neg	pos	pos	pos	ND	ND	ND	pos
5	F	LyP	23	pos	pos	ND	neg	neg	pos	ND	pos	ND	ND	ND	pos
6	F	C-ALCL	50	pos	pos	ND	neg	neg	pos	ND	ND	ND	ND	ND	ND
7	M	C-ALCL	33	pos	pos	ND	neg	neg	pos	ND	ND	ND	ND	ND	ND
8	M	C-ALCL	89	pos	pos	pos	neg	neg	pos	pos	pos	ND	neg	neg	ND
9	M	C-ALCL	70	pos	pos	ND	ND	neg	pos	pos	ND	pos	ND	ND	ND
10	M	C-ALCL	65	Pos	pos	ND	ND	neg	pos	ND	ND	ND	ND	ND	ND

Abbreviations: C-ALCL, cutaneous anaplastic large cell lymphoma; DX, diagnosis; F, female; GB, Granzyme B; LyP, lymphomatoid papulosis; M, male; ND, not done; neg, negative; Pf, Perforin; pos, positive.

Cases 1a (biopsy performed in April 2018) and case 1b (biopsy performed in November 2018) are from the same patient. All specimens are ALK negative (not shown).

In our cohort of patients, the male:female ratio was 3:2 for LyP and 4:1 for C-ALCL. Almost all patients were diagnosed after 2008 except for one patient whose initial diagnosis was in 1971. Lesions in both patient subtypes showed no predilection for any single area of the skin surface. Three of the five patients diagnosed with LyP were treated with skin-directed therapy, whereas the remaining two needed therapy with systemic, low-dose methotrexate. Of the patients with C-ALCL, three required systemic therapy owing to extensive, relapsing disease, whereas two required skin-directed therapy alone.

The overall survival of patients with LyP and C-ALCL was excellent, with all patients diagnosed with LyP alive to date. Of the patients with C-ALCL, one of the five patients died, but this was not due to the disease.

A histologic review showed that all cases of C-ALCL had >75% of the cells with large, anaplastic cells in sheets. In cases of LyP, all met the criteria for histologic subtypes A or C (Swerdlow et al., 2017). With regard to immunohistochemistry (IHC), all cases were positive for CD3, CD4, and CD30 with loss of CD7. CD8 was negative in all cases. All cases of C-ALCL were negative for ALK-1. Only two cases of LyP were tested for ALK-1 IHC, and both were found to be negative. Regarding cytotoxic markers, three of the six LyP cases and two of the five C-ALCL cases were positive for one of the three cytotoxic markers (TIA-1, perforin, and/or granzyme) (Table 1). All cases except one did not have IHC performed for TCR-delta.

Genomic landscape of LyP and C-ALCL

The sample size is small, reflecting the rarity of the disease even at tertiary referral centers. However, we observed recurrent mutations displaying overlap with other lymphomas in epigenetic modifying genes, the Jak/signal transducer and activator of transcription (STAT) pathway, and the T-cell signaling pathway.

All cases of CD30$^+$LPDs had recurrent mutations in at least one of the epigenetic modifying genes, with the most frequent mutations found in the mixed lineage methyltransferase family involved in the methylation of H3K4: *CREBBP* (n = 3, 27%), *KMT2A* (n = 4, 36%), *KMT2D* (n = 4, 36%), *SETD2* (n = 3, 27%), and *SMARCA4* (n = 3, 27%) (Figure 1). Specific H3K4 methyltransferase mutations included *KMT2A* (p.482H, p.S3479X [stopgain], p.P1279T) (n = 3, 27%), *KMT2D* (p.P2230Q, p.L978P) (n = 2, 18%), and *KMT2C* (p.P3598T) (n = 1, 9%). We also noted mutations in the SET domain such as *SETD2* (p.R1548X [stopgain], p.E2128D, p.K2360N) (n = 3, 27%), *SETD4* (p.P121T) (n = 1, 9%), *SETD5* (p.G486D)(n = 1, 9%), and *SETDB1* (splice-site) (n = 1, 9%).

Within the Jak/STAT pathway, mutations of *STAT3* were observed in two cases of C-ALCL (p.Y640F, p.G656C, SH2 domain) (n = 2, 18%), those of *STAT5B* was found in one case of LyP (p.S420Y, STAT-binding domain) (n = 1, 9%), and *Jak1* mutation was found in one case of LyP (p.F286C, FERM domain) (n = 1, 9%).

Mutations were also identified in the T-cell signaling and activation pathway. Three of the five cases of C-ALCL showed loss-of-function mutations (p.S493Y, p.P21Q, p.S652X) in *EOMES,* a T-box transcription factor important in lymphocyte development (McLane et al., 2013). We had two cases of C-ALCL and one case of LyP with *NOTCH1* mutations, supporting the importance of this gene in T-cell lymphomas. There was one case of C-ALCL and two cases of LyP with mutations in *IRF4*.

We also had copy number (CN) analysis on nine cases of CD30$^+$LPD (six LyP and three C-ALCL), and none of them showed CN loss of *TP53* or *CDKN2A*–*CDKN2B* compared with that in the normal, supporting the findings of other studies that the lack of these abnormalities may be associated with indolent behavior (Laharanne et al., 2010) (Figure 2). We also did not observe recurrent CN aberrations of genes in the Jak/STAT pathway or epigenetic regulators.

DISCUSSION

The etiology, pathogenesis, and molecular characteristics of LyP and C-ALCL remain largely unknown (Swerdlow et al., 2017). Although multiple molecular changes, including chromosomal, genomic, and gene expression aberrations as well as altered microRNA expression and methylation patterns have been described for the histologic mimics of CD30$^+$LPDs, little is known about the molecular profile of

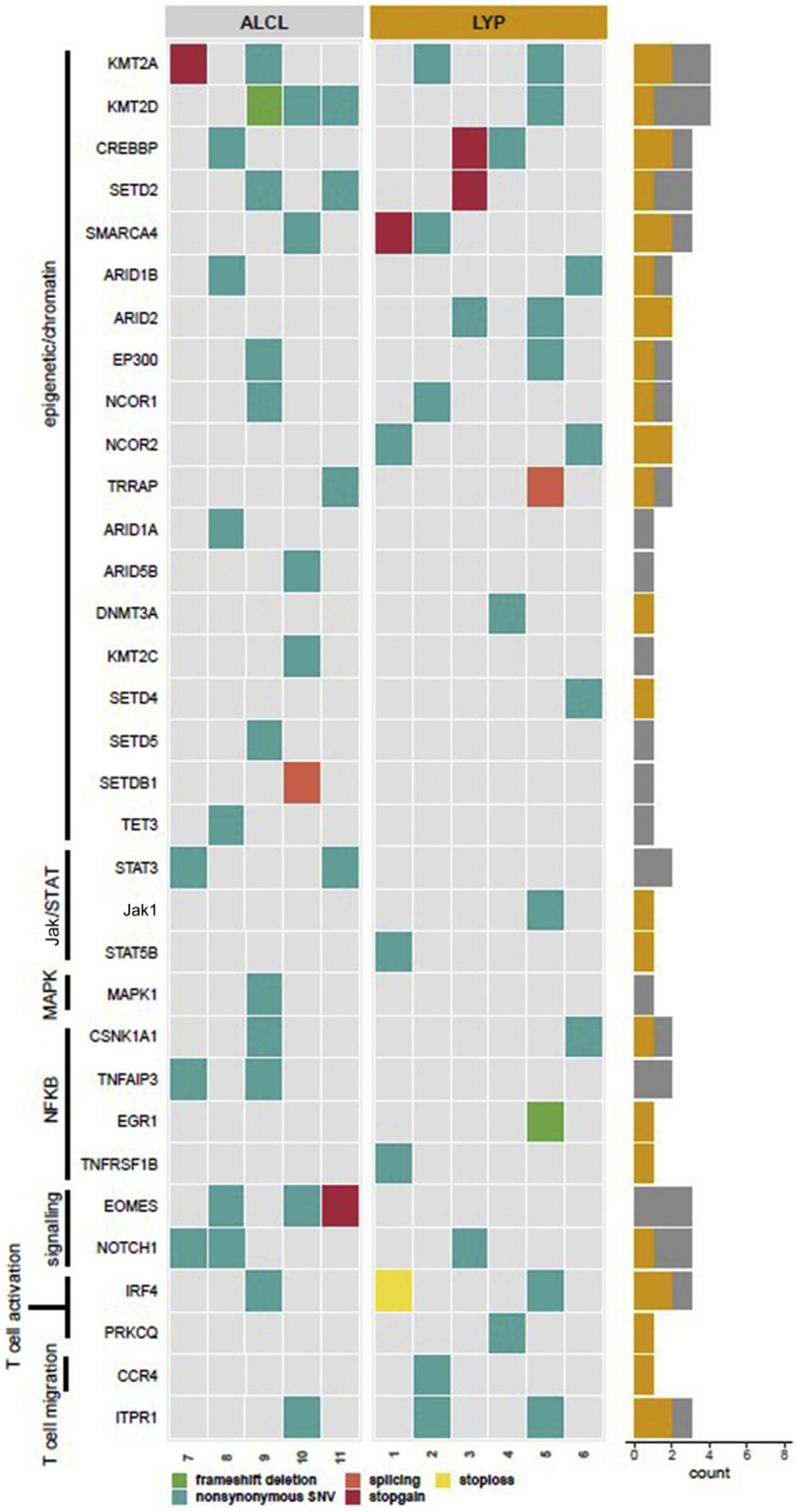

Figure 1. Whole-exome sequencing of C-ALCL and LyP with frequent mutations related to specific pathways. ALCL, anaplastic large cell lymphoma; C-ALCL, cutaneous anaplastic large cell lymphoma; LYP, lymphomatoid papulosis; STAT, signal transducer and activator of transcription.

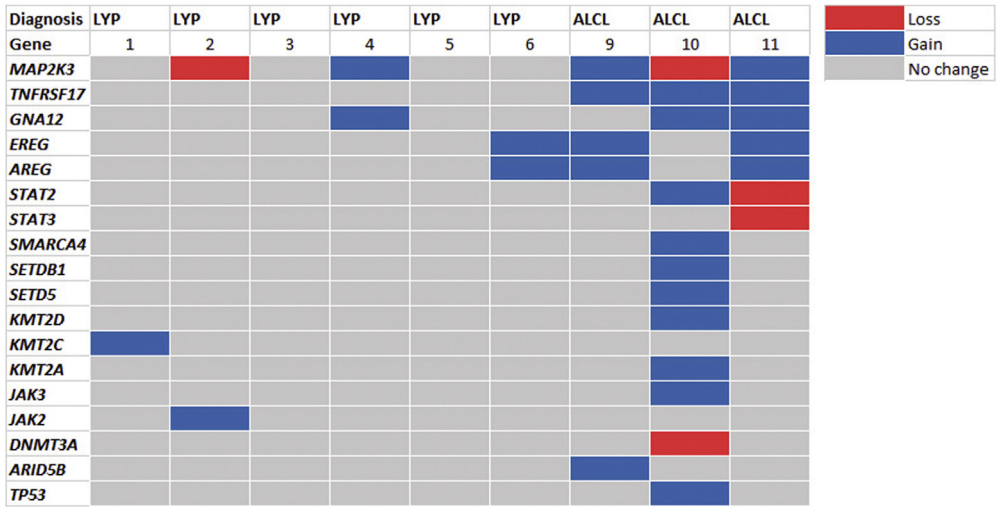

Figure 2. Copy number analysis of pertinent genes related to cutaneous lymphoma. ALCL, anaplastic large cell lymphoma; LYP, lymphomatoid papulosis.

LyP or C-ALCL. This serves as a barrier to the differentiation among these entities, with continued reliance on clinical interpretation rather than on the use of genetic information for diagnosis or therapeutic intervention.

Although our sample size is small, reflecting the rarity of the disease even at tertiary referral centers, we noted recurrent mutations in several pathways. CD30$^+$LPD is a subtype of CTCL; hence, we compared our data with those of other types of CTCL, MF, and Sezary syndrome. The mutational landscape showed overlap most notably in the Jak/STAT pathway, with mutations in *Jak1*, *STAT3*, and *STAT5B* and the epigenetic modifying genes of *CREBBP*, *KMT2C*, and *KMT2D* (Supplementary Table S1) (Choi et al., 2015; Kiel et al., 2015; McGirt et al., 2015; Ungewickell et al., 2015; Woollard et al., 2016). All our LyP and C-ALCL samples in this study had recurrent mutations in epigenetic modifying genes affecting histone methylation and acetylation. In particular, they harbored frequent mutations related to the mixed lineage methyltransferase family involved in the methylation of *H3K4*, which is important in regulating gene transcription. Many of the same mutations in epigenetic and histone modification genes such as *KMT2D*, *KMT2A*, *SETD2*, and *CREBBP* noted in our population are also seen in peripheral T-cell lymphoma and breast implant–associated anaplastic large cell lymphoma (BI-ALCL) (Ji et al., 2018). Whole-exome sequencing of a large series of BI-ALCL showed recurrent mutations in similar epigenetic regulators in 74% of cases, involving notably *KMT2C* (26%), *KMT2D* (9%), *CHD2* (15%), and *CREBBP* (15%) (Laurent et al., 2020). The overlap of BI-ALCL with CD30$^+$LPD is interesting because the histologic and immunophenotypic findings of both entities are very similar, as is the relatively indolent behavior of both. However, *KMT2D* mutations are also seen in more aggressive diseases as well such as mixed lineage leukemia, acute myeloid leukemia, and non-Hodgkin lymphoma. In mixed lineage leukemia, *KMT2D* interacts directly with *p53* to promote the expression of *p53* target genes (Rao and Dou, 2015). It is postulated that loss-of-function *KMT2D* mutations promote tumorigenesis through the dysregulation of enhancer activity regulated by tumor suppressors (e.g., p53) and oncogenes (e.g., *MYC*), perhaps leading to more aggressive disease. In addition, recent work by Lobello et al. (2019) noted *KMT2D* mutations as well as *TP53* in patients with sALCL. Prognostically, the most recurrent genes mutated in patients with a dismal outcome in their study of 275 cases (dead and/or relapsed patients) were *TP53*, *STAT3*, and *Jak1*. Of note, although *TP53* can be mutated in other forms of CTCL, such as MF and Sezary syndrome as well as sALCL, that was not seen in our cases.

Interestingly, the loss-of-function mutation in *SETD2* noted in both LyP and C-ALCL are similar to those seen in enteropathy-associated T-cell lymphoma and hepatosplenic T-cell lymphoma (Moffitt et al., 2017) but is uncommon in other CTCLs such as cutaneous gamma-delta T-cell lymphoma and BI-ALCL (Choi et al., 2015; Laurent et al., 2020; Park et al., 2017). Loss of *SETD2* leads to an expansion of γδ T cells, which is the primary cell type in enteropathy-associated T-cell lymphoma and hepatosplenic T-cell lymphoma (Skucha et al., 2019). Several cases of LyP have been reported to carry a γδ phenotype (Morimura et al., 2011). However, in our small set of cases, the tissue samples were exhausted, prohibiting a standard examination of this IHC, particularly in the cases carrying a *SETD2* mutation.

The Jak/STAT pathway is involved with cytokine signaling, proliferation of healthy T lymphocytes, and the differentiation of T helper cell subsets. In this study, mutations in this pathway were identified in both LyP (*Jak1, STAT5B*) and C-ALCL (*STAT3*). Mutations as well as CN alterations of *Jak2*, *STAT3*, and *STAT5B* have been reported in MF/Sezary syndrome (Choi et al., 2015; Eriksen et al., 2001). Alteration of the Jak/STAT pathway in malignant CTCL cells is postulated to play a role in their differentiation into T helper type 2 or regulatory T cell subtypes. *STAT3* and *Jak1* have also been found to be mutated solely in ALK-negative sALCL (as opposed to ALK positive), the major histologic mimic of CD30$^+$LPD (Lobello et al., 2019). Mutations in *STAT3* were more recurrent in ALK-negative patients with ALCL, with shorter overall survival. BI-ALCL also displays gain-of-function mutations in this pathway, including *STAT3* (38%), *Jak1* (18%), and *STAT5B* (3%), and in negative regulators,

including *SOCS3* (6%), *SOCS1* (3%), and *PTPN1* (3%). All BI-ALCLs expressed phosphorylated STAT3 on immunohistochemical staining, regardless of the mutational status of genes in the Jak/STAT pathway.

EOMES is a T-box transcription factor important for both the function and homeostasis of effector and memory T cells as well as lymphocyte development and differentiation (McLane et al., 2013). In our series, *EOMES* was mutated, resulting in a loss of function in 60% of C-ALCL but in none of the cases of LyP. Genomic alterations, particularly in-frame insertion–deletion, in *EOMES* has also been noted in 18% of cases of BI-ALCL (Laurent et al., 2020). A study by Intlekofer et al. (2005) showed that *Tbx21* and *EOMES* have a cooperative function that is important to the cytotoxic programming of T cells and that mutations or deletions in these genes lead to a defective cytotoxic program. *NOTCH1* mutations were also seen in two cases of C-ALCL and in one case of LyP. *Notch1* appears to play an important role in C-ALCL (Kamstrup et al., 2008) and sALCL with activating mutations, particularly in the heterodimerization or PEST domain (Weng et al., 2004). We also identified one case of C-ALCL and two cases of LyP with mutations in *IRF4*. *IRF4* is an important gene for T-cell activation, and the translocation with *DUSP22* has been detected in cases of C-ALCL and sALCL (Luchtel et al., 2018). Mutations of *IRF4* are commonly seen in adult T-cell lymphoma/leukemia and are believed to be a major downstream target of NF-kB (Kataoka et al., 2015).

Of note, the major histologic mimic of $CD30^+$LPD, ALK-negative sALCL, has an aggressive course necessitating systemic therapy. Hence, the differential of these entities is important. Although there is overlap with $CD30^+$LPD-harboring mutations in *STAT3* and *Jak1*, which are mutated in the ALK–sALCL, other recurrently mutated genes such as *TP53, EPHA5, LRP1B, PRDM1*, and *SOCS1* were not found in our study of $CD30^+$LPD. Mutations in *STAT3* were more recurrent in patients with ALK–sALCL with shorter overall survival, and clones harboring mutated *TP53* were detectable more often in relapsed Salcl, thereby suggesting a possible driving role (Lobello et al., 2019). Genes involved in cell cycle control and apoptosis, such as *TP53*, although frequently mutated in other cutaneous lymphomas such as MF and Sezary syndrome, were not noted in our cohorts (Choi et al., 2015; Karenko et al., 2007; Laharanne et al., 2010; McGirt et al., 2015). *TP53* mutation is more characteristic of aggressive and advanced cutaneous lymphomas, which may explain its absence in more indolent LyP and C-ALCL.

Genomic characterization of LyP and C-ALCL in this series confirms the role of multiple pathways that overlap not only with cutaneous lymphoma but also with other systemic lymphomas. However, although the Jak/STAT pathway and epigenetic alterations possibly play a role in the pathogenesis of these diseases, genes involved in cell cycle control and apoptosis (i.e., *TP53, PLCG1*) that are characteristic of more aggressive diseases were not identified and may support the indolent behavior of these cases. Extending this investigation to a larger number of samples will allow us to confirm these findings and identify additional mutations that may help distinguish $CD30^+$LPD from other histologic mimics of this disease spectrum and identify, to our knowledge, previously unreported targets for therapy.

Table 2. Immunohistochemical Stains and the Clones that Were Used for Routine Staining of Cutaneous T-cell Lymphomas

Antibody	Clone	Vendor
CD3	2GV6	Ventana, Tucson, AZ
CD4	SP35	Ventana, Tucson, AZ
CD7	SP94	Ventana, Tucson, AZ
CD8	SP57	Ventana, Tucson, AZ
CD30	Ber-H2	Dako Laboratories, Carpinteria, CA
CD5	SP19	Ventana, Tucson, AZ
CD20	L26	Ventana, Tucson, AZ
TIA-1	2G9A10F5	Beckman Coulter, Fullerton, CA
Granzyme	Polyclonal	Ventana, Tucson, AZ
Perforin	MRQ-23	Ventana, Tucson, AZ
Beta-F1	8A3	Thermo Fisher Scientific, Waltham, MA
TCR-Delta	H-41	Santa Cruz Antibodies, Santa Cruz, CA
Ki-67	30-9	Ventana, Tucson, AZ
ALK-1	ALK01	Ventana, Tucson, AZ

MATERIALS AND METHODS

Institutional Review Board approval was obtained at each institution. A waiver of informed consent was approved by the Institutional Review Board for use of the archived material. The clinical and pathologic information associated with each case were reviewed centrally at the City of Hope National Medical Center to confirm the rendered diagnosis by dermatologists (CQ and FA), dermatopathologists (FA, CQ, VP), and a hematopathologist (JS). IHC was performed on 3–4-micron sections of formalin-fixed, paraffin-embedded (FFPE) tissue using antibodies to CD3, CD4, CD7, CD8, and CD30. The slides were stained on the Ventana Discovery XT platform (Ventana, Tucson, AZ) and on a Leica Bond III instrument (Leica Biosystems, Chicago, IL). In the course of clinical diagnostics, some cases had stains performed for CD5, CD20, TIA-1, granzyme, perforin, Beta F-1, TCR-Delta, Ki-67, and ALK-1 (Table 2). FFPE tissue blocks were used to create new slides and to isolate neoplastic and non-neoplastic areas of tissue for genomic analysis.

Mutation analysis

Archived specimens with paired normal tissue were analyzed by whole-exome sequencing. For FFPE tissue blocks, typical collection and handling procedures for genomic analysis include cutting approximately 20 microtome sections at 5-micron thickness each on uncoated slides and staining the first and last recut slides with H&E. DNA was extracted using the Qiagen DNA FFPET kit (Qiagen, Valencia, CA), following the manufacturer's instructions. The tumor DNA and matched normal were submitted for whole-exome sequencing at the City of Hope National Medical Center Integrative Genomics Core. FFPE DNA samples were sheared on the Covaris E220 Focused ultrasonicator (Covaris, Woburn, MA) to a fragment size of 150–200 bp, and about 200 ng of genomic DNA was repaired using NEBNext FFPE DNA Repair Mix. The repaired DNA was quantified by Qubit and converted to precapture DNA libraries using Kapa HyperPrep Kit. Whole-exome regions of genomic DNA were enriched with Agilent's SureSelect All exon V6+COSMIC Baits. The quality and concentration of enriched libraries were evaluated using Agilent 2200 Bioanalyzer with high

sensitivity DNA kit and Qubit 2.0 Fluorometer. Enriched libraries were subjected to paired-end 100 bp sequencing using a HiSeq 2500 to achieve ×50 coverage. Initial correlative and descriptive analyses were performed on archival tissue to discover the genomic signatures unique to each disease entity. Genomic profiles of these entities were compared with those of matched normal skin specimens in all cases. For whole-exome sequencing data, raw sequencing reads were aligned to the human reference genome hg38 using Burrows–Wheeler Aligner (version 0.7); duplicate marking and indel realignment were conducted using Picard (version 2.9), and the base quality was recalibrated using Genome Analysis Toolkit (version 4.1). Variant calling was performed using two variant callers: VarScan (version 2.4) and Genome Analysis Toolkit (version 4.1) Mutect2, with somatic mode using paired normal and tumor samples. ANNOVAR was used for variant annotation against public databases such as COSMIC, version 83; gnomAD; and ClinVar. Variants affecting the coding region or splice sites were retained. We then kept variants that had variant allele frequency in the tumor sample of at least 5%, with more than four reads supporting variant allele plus at least one read supporting forward and reverse strands. Next, we merged the variants called by the two variant callers and filtered out the variants with minor allele frequency over 1% and that were not expressed in normal T cells using in-house gene expression profiling data. The interpretation databases were used to determine the importance of the variants. We rescued variants using looser criteria if the genes were reported in other studies for further investigation. Somatic CN analysis was conducted using Bioconductor package TitanCNA. Various types of structural variations, including large insertions/deletions, inversions, and translocations, were identified using Pindel and Lumpy.

We then compared our CD30+ LPD genomic profile with published datasets of other cutaneous lymphomas with the goal of identifying unique profiles that would help to differentiate these entities.

CN analysis

Calculation of read coverage, correction of guanine-cytosine content and mappability biases, and data segmentation were (Ha et al., 2014) performed at 50 kb bins across the genome using ichorCNA, version 0.3.2 (Adalsteinsson et al., 2017). TitanCNA, version 1.24.0, with recommended parameters for exome sequencing, and GISTIC2, version 2.0.23 (Mermel et al., 2011), with confident level 0.9, were used to identify CN variations using ichorCNA-generated segments. Significant regions of CN alteration that are $\log_2$ CN ratio >0.1 or < -0.1 were selected from identified CN alterations. Overlapped significant regions between detected CN events by TitanCNA and GISTIC2 remained for annotation. Annotation of CN variation was accomplished using AnnotSV, version 3.0.5 (Geoffroy et al., 2018).

Data availability statement

Datasets related to this article can be found at https://www.ncbi.nlm.nih.gov/sra, hosted at Sequence Read Archive under submission SUB8951650. (https://www.ncbi.nlm.nih.gov/bioproject/PRJNA695786).

ORCIDs

Farah R. Abdulla: http://orcid.org/0000-0002-3455-7566
Weiwei Zhang: http://orcid.org/0000-0002-6123-8034
Xiwei Wu: http://orcid.org/0000-0002-7071-1671
Kord Honda: http://orcid.org/0000-0002-2936-7573
Hanjun Qin: http://orcid.org/0000-0002-0370-0913
Hyejin Cho: http://orcid.org/0000-0002-9954-8118
Christiane Querfeld: http://orcid.org/0000-0001-9698-5809
Jasmine Zain: http://orcid.org/0000-0003-4308-629X
Steven Terry Rosen: http://orcid.org/0000-0002-8818-7724
Wing C. Chan: http://orcid.org/0000-0002-6243-6008
Vishwas Parekh: http://orcid.org/0000-0003-3131-2958
Joo Y. Song: http://orcid.org/0000-0003-3497-2513

AUTHOR CONTRIBUTIONS

Conceptualization: FRA, JYS; Data Curation: FRA, JYS, VP, KH, HQ, WZ; Formal Analysis: FRA, XW, HQ, WZ, WC; Funding Acquisition: FRA; Investigation: FRA, JYS, XW, VP; Methodology: FRA, JYS; Project Administration: FRA; Resources: XW; Software: XW, WZ; Supervision: STR, WC, FRA, JZ, CQ; Validation: FRA, JYS, WZ; Visualization: FRA, JYS, WZ; Writing - Original Draft Preparation: FRA, JYS, WZ; Writing - Review and Editing: JYS, XW, VP, HQ, FRA, WZ, STR, WC, CQ, JZ

Disclaimer

The content of this study is solely the responsibility of the authors and does not necessarily represent the official views of the National Institutes of Health (Bethesda, MD).

ACKNOWLEDGMENTS

For Core Facilities at the City of Hope, the research reported in this publication included work performed in the Integrative Genomics Core supported by the National Cancer Institute of the National Institutes of Health (Bethesda, MD) under grant number P30CA033572. For Pilot Projects and Early Phase Clinical Research Support, the research reported in this publication was supported by the National Cancer Institute of the National Institutes of Health under grant number P30CA033572.

CONFLICT OF INTEREST

VP is a consultant for Genentech. CQ is on the advisory board/steering committee for Helsinn, Kyowa Kirin, Bioniz, Miragen, Trillium, and Mallinckrodt and on speakers Bureau for Helsinn and is funded by Celgene. JZ is consulting for Seagen, Verastem, Curio, Kiyowa Kirin, and Mundi Pharma and is on speakers Bureau for Seagen, Kiyowa Kirin and received support from Seattle Genetics and Secura Bioresearch. The remaining authors state no conflict of interest.

SUPPLEMENTARY MATERIAL

Supplementary material is linked to the online version of the paper at www.jidonline.org, and at https://doi.org/10.1016/j.xjidi.2021.100068.

REFERENCES

Adalsteinsson VA, Ha G, Freeman SS, Choudhury AD, Stover DG, Parsons HA, et al. Scalable whole-exome sequencing of cell-free DNA reveals high concordance with metastatic tumors. Nat Commun 2017;8:1324.

Choi J, Goh G, Walradt T, Hong BS, Bunick CG, Chen K, et al. Genomic landscape of cutaneous T cell lymphoma. Nat Genet 2015;47:1011–9.

Eriksen KW, Kaltoft K, Mikkelsen G, Nielsen M, Zhang Q, Geisler C, et al. Constitutive STAT3-activation in Sezary syndrome: tyrphostin AG490 inhibits STAT3-activation, interleukin-2 receptor expression and growth of leukemic Sezary cells. Leukemia 2001;15:787–93.

Feldman AL, Dogan A, Smith DI, Law ME, Ansell SM, Johnson SH, et al. Discovery of recurrent t(6;7)(p25.3;q32.3) translocations in ALK-negative anaplastic large cell lymphomas by massively parallel genomic sequencing. Blood 2011;117:915–9.

Geoffroy V, Herenger Y, Kress A, Stoetzel C, Piton A, Dollfus H, et al. AnnotSV: an integrated tool for structural variations annotation. Bioinformatics 2018;34:3572–4.

Ha G, Roth A, Khattra J, Ho J, Yap D, Prentice LM, et al. TITAN: inference of copy number architectures in clonal cell populations from tumor whole-genome sequence data. Genome Res 2014;24:1881–93.

Intlekofer AM, Takemoto N, Wherry EJ, Longworth SA, Northrup JT, Palanivel VR, et al. Effector and memory CD8+ T cell fate coupled by T-bet and eomesodermin [published correction appears in Nat Immunol 2006;7:113]. Nat Immunol 2005;6:1236–44.

Ji MM, Huang YH, Huang JY, Wang ZF, Fu D, Liu H, et al. Histone modifier gene mutations in peripheral T-cell lymphoma not otherwise specified. Haematologica 2018;103:679–87.

Kamstrup MR, Ralfkiaer E, Skovgaard GL, Gniadecki R. Potential involvement of Notch1 signalling in the pathogenesis of primary cutaneous CD30-positive lymphoproliferative disorders. Br J Dermatol 2008;158:747–53.

Karai LJ, Kadin ME, Hsi ED, Sluzevich JC, Ketterling RP, Knudson RA, et al. Chromosomal rearrangements of 6p25.3 define a new subtype of lymphomatoid papulosis. Am J Surg Pathol 2013;37:1173–81.

Karenko L, Hahtola S, Ranki A. Molecular cytogenetics in the study of cutaneous T-cell lymphomas (CTCL). Cytogenet Genome Res 2007;118:353–61.

Kataoka K, Nagata Y, Kitanaka A, Shiraishi Y, Shimamura T, Yasunaga J, et al. Integrated molecular analysis of adult T cell leukemia/lymphoma. Nat Genet 2015;47:1304–15.

Kempf W, Pfaltz K, Vermeer MH, Cozzio A, Ortiz-Romero PL, Bagot M, et al. EORTC, ISCL, and USCLC consensus recommendations for the treatment of primary cutaneous CD30-positive lymphoproliferative disorders: lymphomatoid papulosis and primary cutaneous anaplastic large-cell lymphoma. Blood 2011;118:4024–35.

Kiel MJ, Sahasrabuddhe AA, Rolland DCM, Velusamy T, Chung F, Schaller M, et al. Genomic analyses reveal recurrent mutations in epigenetic modifiers and the JAK-STAT pathway in Sézary syndrome. Nat Commun 2015;6:8470.

Laharanne E, Chevret E, Idrissi Y, Gentil C, Longy M, Ferrer J, et al. CDKN2A–CDKN2B deletion defines an aggressive subset of cutaneous T-cell lymphoma. Mod Pathol 2010a;23:547–58.

Laharanne E, Oumouhou N, Bonnet F, Carlotti M, Gentil C, Chevret E, et al. Genome-wide analysis of cutaneous T-cell lymphomas identifies three clinically relevant classes. J Invest Dermatol 2010b;130:1707–18.

Laube S, Shah F, Marsden J. Consequences of misdiagnosis of lymphomatoid papulosis. Eur J Cancer Care (Engl) 2006;15:194–8.

Laurent C, Nicolae A, Laurent C, Le Bras F, Haioun C, Fataccioli V, et al. Gene alterations in epigenetic modifiers and JAK-STAT signaling are frequent in breast implant-associated ALCL. Blood 2020;135:360–70.

Lobello C, Tichý B, Bystrý V, Radova L, Filip D, Mraz M, et al. Analysis of mutational landscape in systemic anaplastic large cell lymphoma identifies novel prognostic markers. Blood 2019;134(Suppl. 1):1490.

Luchtel RA, Dasari S, Oishi N, Pedersen MB, Hu G, Rech KL, et al. Molecular profiling reveals immunogenic cues in anaplastic large cell lymphomas with *DUSP22* rearrangements. Blood 2018;132:1386–98.

McGirt LY, Jia P, Baerenwald DA, Duszynski RJ, Dahlman KB, Zic JA, et al. Whole-genome sequencing reveals oncogenic mutations in mycosis fungoides. Blood 2015;126:508–19.

McLane LM, Banerjee PP, Cosma GL, Makedonas G, Wherry EJ, Orange JS, et al. Differential localization of T-bet and Eomes in CD8 T cell memory populations. J Immunol 2013;190:3207–15.

Mermel CH, Schumacher SE, Hill B, Meyerson ML, Beroukhim R, Getz G. GISTIC2.0 facilitates sensitive and confident localization of the targets of focal somatic copy-number alteration in human cancers. Genome Biol 2011;12:R41.

Moffitt AB, Ondrejka SL, McKinney M, Rempel RE, Goodlad JR, Teh CH, et al. Enteropathy-associated T cell lymphoma subtypes are characterized by loss of function of SETD2. J Exp Med 2017;214:1371–86.

Morimura S, Sugaya M, Tamaki Z, Takekoshi T, Sato S. Lymphomatoid papulosis showing γδ T-cell phenotype. Acta Derm Venereol 2011;91:712–3.

Park J, Yang J, Wenzel AT, Ramachandran A, Lee WJ, Daniels JC, et al. Genomic analysis of 220 CTCLs identifies a novel recurrent gain-of-function alteration in RLTPR (p.Q575E). Blood 2017;130:1430–40.

Rao RC, Dou Y. Hijacked in cancer: the KMT2 (MLL) family of methyltransferases. Nat Rev Cancer 2015;15:334–46.

Skucha A, Ebner J, Grebien F. Roles of SETD2 in leukemia-transcription, DNA-damage, and beyond. Int J Mol Sci 2019;20:1029.

Swerdlow S, Campo E, Harris NL, Jaffe ES, Pileri SA, Stein H, et al. WHO classification of tumours of haematopoietic and lymphoid tissues. Lyon, France: International Agency for Research on Cancer; 2017.

Ungewickell A, Bhaduri A, Rios E, Reuter J, Lee CS, Mah A, et al. Genomic analysis of mycosis fungoides and Sézary syndrome identifies recurrent alterations in TNFR2. Nat Genet 2015;47:1056–60.

Velusamy T, Kiel MJ, Sahasrabuddhe AA, Rolland D, Dixon CA, Bailey NG, et al. A novel recurrent NPM1-TYK2 gene fusion in cutaneous CD30-positive lymphoproliferative disorders. Blood 2014;124:3768–71.

Weng AP, Ferrando AA, Lee W, Morris JP 4th, Silverman LB, Sanchez-Irizarry C, et al. Activating mutations of NOTCH1 in human T cell acute lymphoblastic leukemia. Science 2004;306:269–71.

Woollard WJ, Pullabhatla V, Lorenc A, Patel VM, Butler RM, Bayega A, et al. Candidate driver genes involved in genome maintenance and DNA repair in Sézary syndrome. Blood 2016;127:3387–97.